Supporting Information for

A Scalable Ternary SnO_2-Co-C Composite as a High Initial Coulombic Efficiency, Large Capacity and Long Lifetime Anode for Lithium Ion Batteries

Tao Liang[a], Renzong Hu[a], Houpo Zhang[a], Hanyin Zhang[a], Hui Wang[a], Yunpeng Ouyang[b], Jun Liu[a], Lichun Yang[a], and Min Zhu[a]*

[a] Guangdong Provincial Key Laboratory of Advanced Energy Storage Materials, School of Materials Science and Engineering, South China University of Technology, Guangzhou, 510640, China

*E-mail: msrenzonghu@scut.edu.cn

[b] Cell Technology Research Center, Sunwoda Electronic Co., Ltd, Shenzhen 518107,China

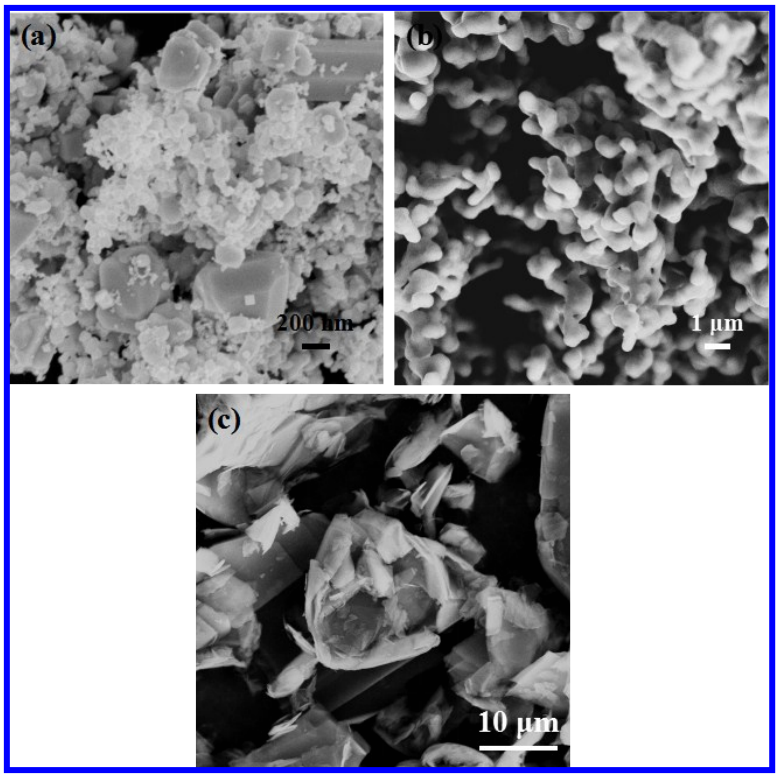

Figure S1 SEM images of pristine (a) SnO_2, (b) Co and (c) graphite, respectively.

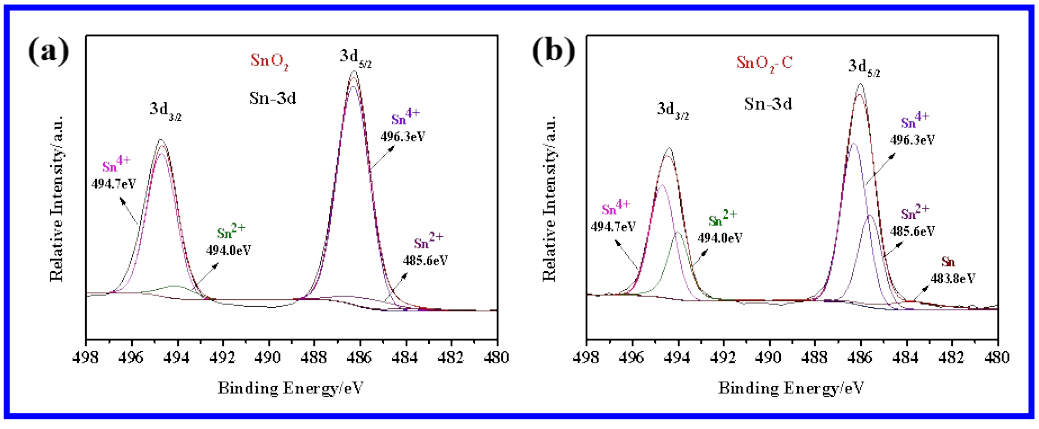

Figure S2 Sn-3d XPS spectra of the milled (a) SnO_2 and (b) SnO_2-C samples.

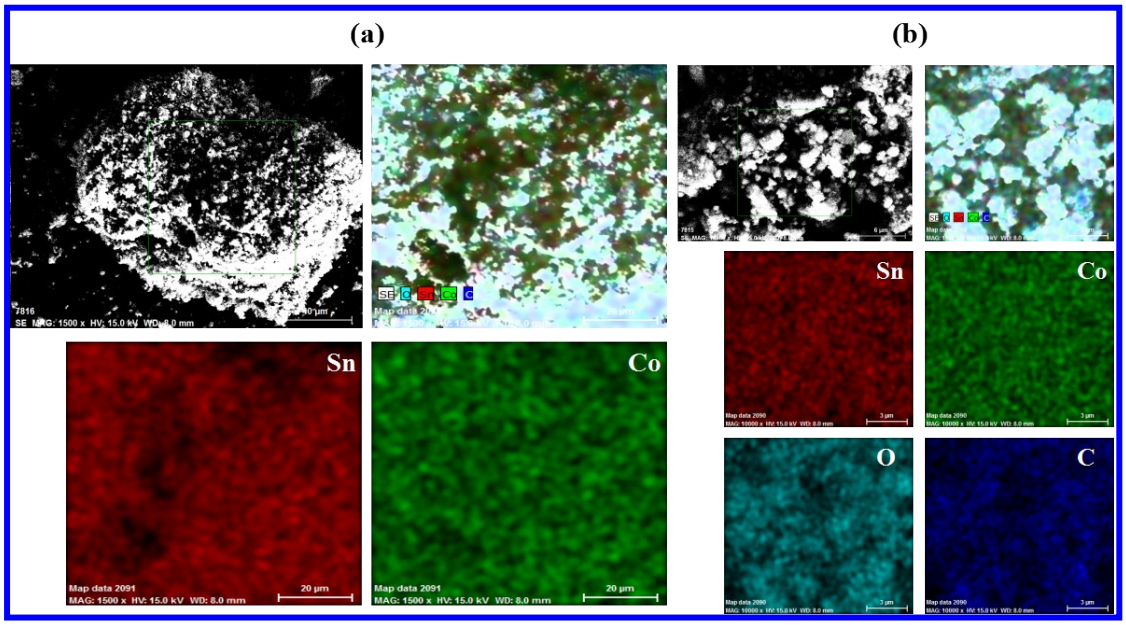

Figure S3 SEM-EDS mapping of the Sn, Co, C and O elements in (a) micro-scale and (b) nano-scale areas of SnO_2-Co-C composite.

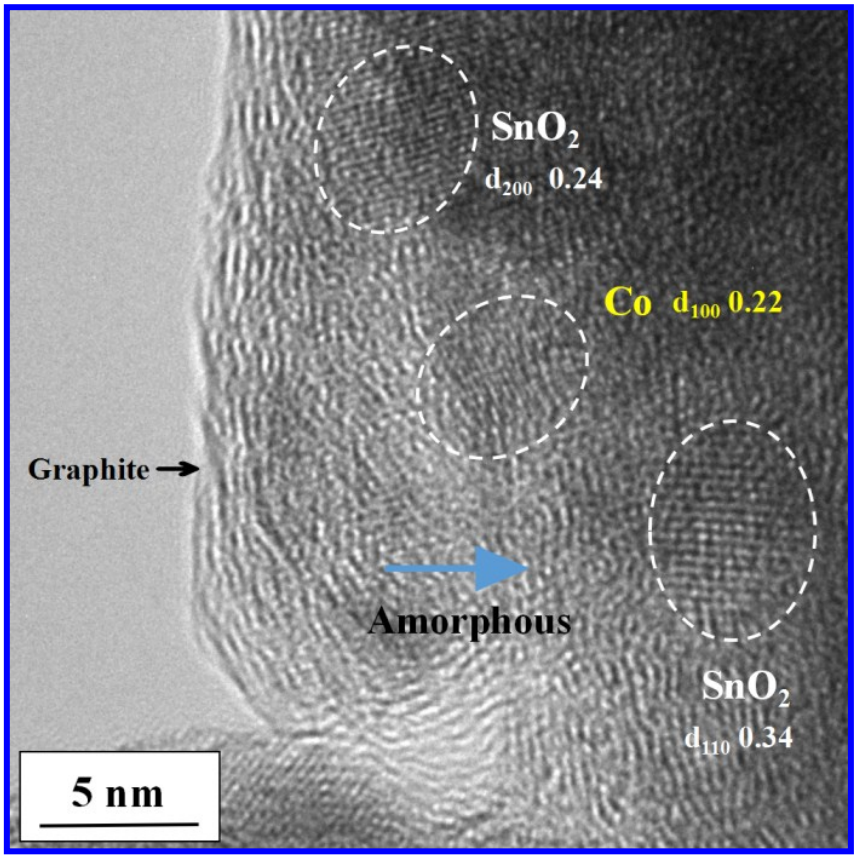

Figure S4 High-resolution image showing the nanosized SnO_2, Mn, amorphous zones and thin graphite nanosheets.

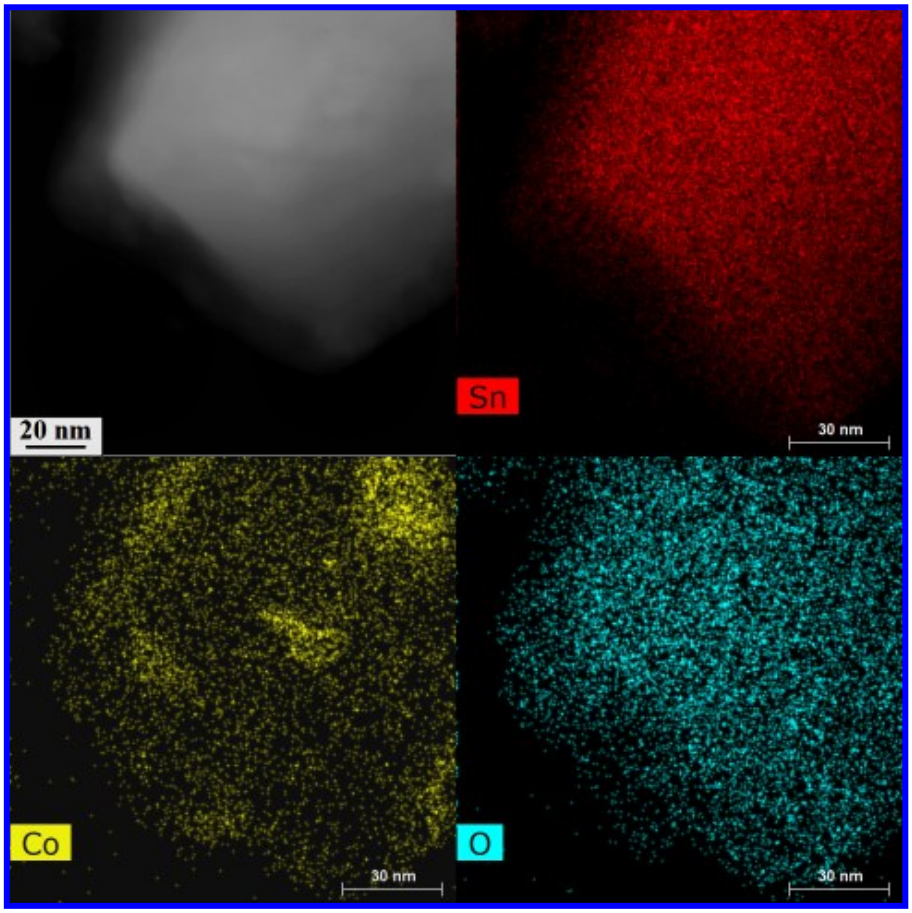

Figure S5 HAADF-STEM image with corresponding elemental mappings of Sn, Co and O in a smaller grain of the SnO_2-Co-C composite.

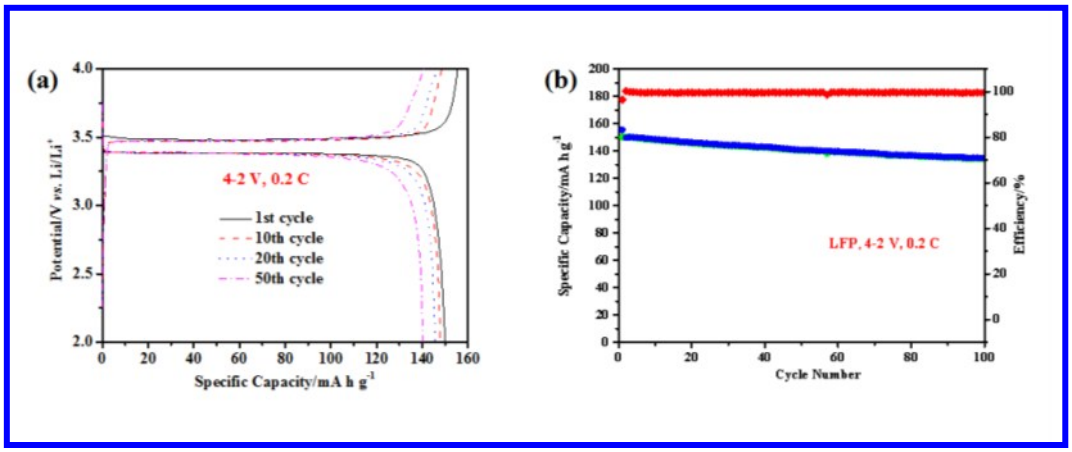

Figure S6 (a) The charge/discharge curves of selective cycles and (b) Cycling performance of commercial $LiFePO_4$ cathode at a current rate of 0.2 C among the potential range of 2-4 V.

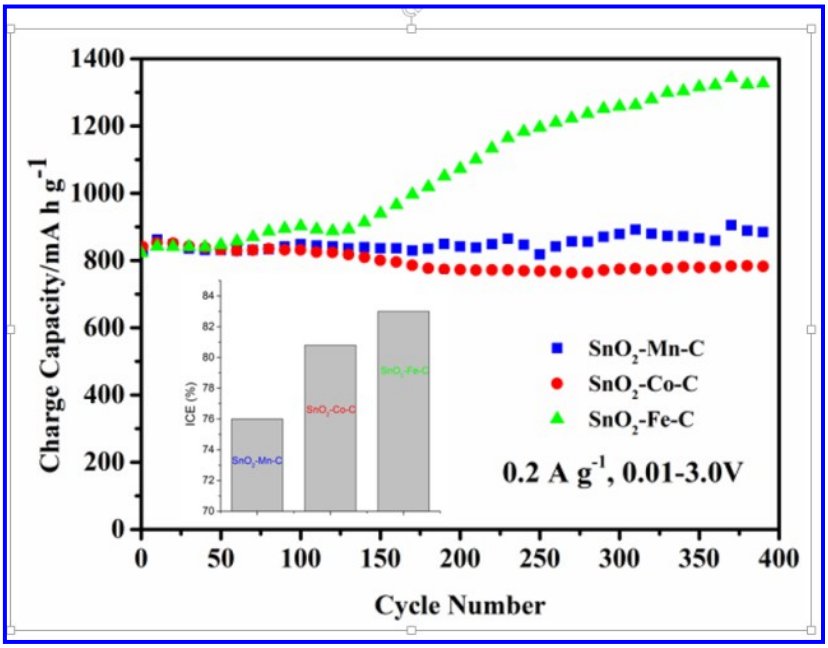

Figure S7 Comparison of the reversible capacity, capacity retention, and ICE of the SnO_2-Mn-C, SnO_2-Fe-C and SnO_2-Co-C composites at a current rate of 0.2 A g^{-1} among potential range of 0.01-3.0 V

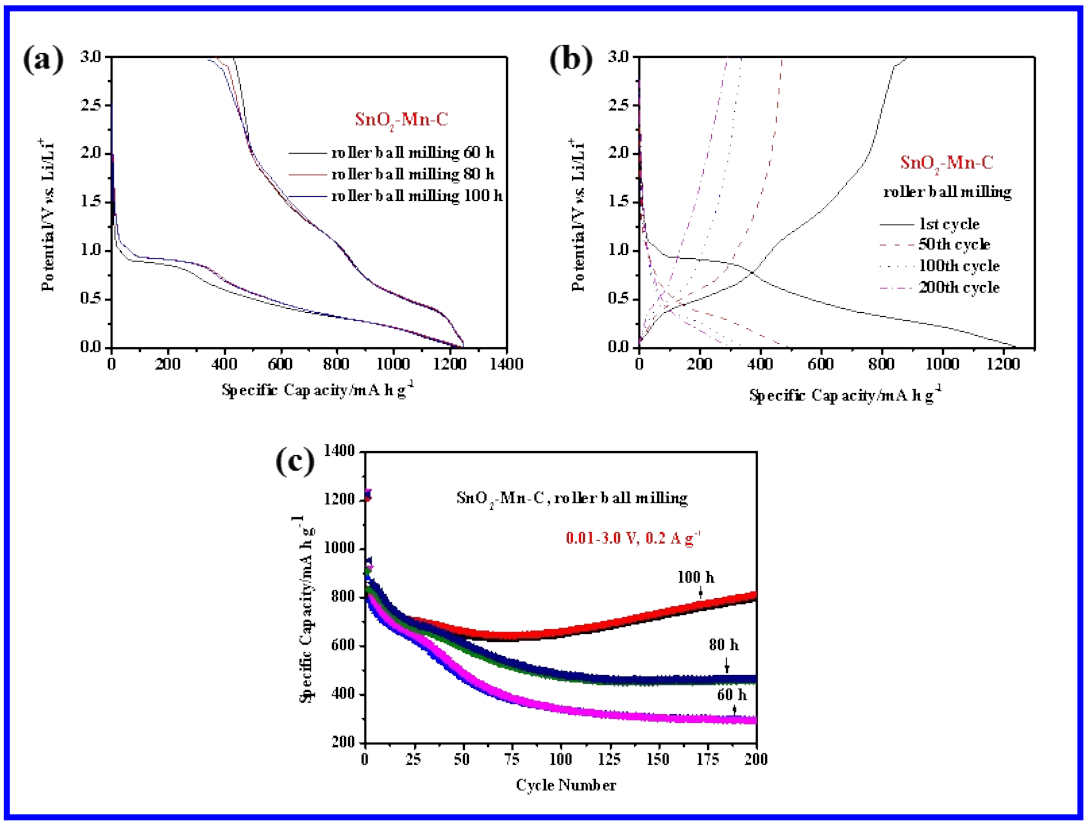

Figure S8 (a) The initial galvanostatic discharge/charge curves of SnO_2-Mn-C prepared by roller ball milling for different time. (b) The selective discharge/charge curves of milled-80 h SnO_2-Mn-C samples at a current rate of 0.2 A g^{-1} among the potential range of 0.01-3.0 V. (c) The cycling performance of the milled SnO_2-Mn-C samples.

Table S1 Comparison of the electrochemical performances of the SnO_2-Co-C ternary anode with other metal oxide nanostructure anodes

	Materials	Synthetic method	Potential range	ICE	1st charge capacity	Capacity retention
Our work	SnO_2-Co-C	ball milling	0.01-3.0 V	80.8 %	894 mA h g^{-1}	780 mA h g^{-1} after 400 cycles at 0.2 A g^{-1} (87.2%)
Ref.S1[1]	SnO_x@C	spray pyrolysis	0.001-3.0 V	65.0 %	1083 mA h g^{-1}	870 mA h g^{-1} after 100 cycles at 2 A g^{-1} (80.3%)
Ref.S2[2]	SnO_2@Co_3O_4 spheres	hydrothermal method	0.05-3.0 V	65.6 %	1167 mA h g^{-1}	815 mA h g^{-1} after 100 cycles at 0.2 A g^{-1} (69.8%)
Ref.S3[3]	Co-SnO_2 spheres	solvothermal method	0.01-2.0 V	67.6 %	1322 mA h g^{-1}	810 mA h g^{-1} after 50 cycles at 0.78 A g^{-1} (61.3%)
Ref.S4[4]	C-SnO_2-rGO	vacuum annealing	0.005-3.0 V	65.9 %	657 mA h g^{-1}	633 mA h g^{-1} after 100 cycles at 0.2 A g^{-1} (96.3%)
Ref.S5[5]	G/SnO_2-Co_3O_4	hydrothermal method	0.01-3.0 V	66.5 %	2173 mA h g^{-1}	1208 mA h g^{-1} after 100 cycles at 1 A g^{-1} (47.3%)
Ref.S6[6]	GNRs/SnO_2	solvothermal method	0.01-2.5 V	74.3 %	1130 mA h g^{-1}	825 mA h g^{-1} after 50 cycles at 0.1 A g^{-1} (73.0%)
Ref.S7[7]	SnO_2/TiO_2 nanocomposites	solvothermal method	0.01-3.0 V	67.1 %	1173 mA h g^{-1}	487 mA h g^{-1} after 1000 cycles at 2 A g^{-1} (41.5%)
Ref.S8[8]	SnO_2-SiC/G	ball milling	0.01-3.0 V	66.0 %	1450 mA h g^{-1}	670 mA h g^{-1} after 650 cycles at 0.1 A g^{-1} (46.2%)
Ref.S9[9]	SnO_2/C composites	solvothermal method	0.01-1.5 V	44.8 %	916 mA h g^{-1}	511 mA h g^{-1} after 1000 cycles at 1.4 A g^{-1} (55.8%)
Ref.S10[10]	SnO_2/Graphene nanosheets	atomic layer deposition	0.01-3.0 V	61.8 %	1042 mA h g^{-1}	793 mA h g^{-1} after 150 cycles at 0.4 A g^{-1} (76.1%)
Ref.S11[11]	SnO_2@TiO_2	atomic layer	0.005-1.5 V	67.7 %	962 mA h g^{-1}	393 mA h g^{-1} after 1000 cycles at 0.4 A

	core-shell nanowires	deposition				g^{-1} (40.9%)
Ref.S12[12]	N-doped SnO_2 nanoparticles	laser-assisted pyrolysis	0.01-3.0 V	69.0 %	1182 mA h g^{-1}	750 mA h g^{-1} after 500 cycles at 1.4 A g^{-1} (63.5%)
Ref.S13[13]	SnO_2 in N-doped Graphene sheets	vapor reduction method	0.005-3.0 V	61.3 %	1144 mA h g^{-1}	1346 mA h g^{-1} after 500 cycles at 0.5 A g^{-1} (85.0%)
Ref.S14[14]	Co_3O_4/C	electrodeposition	0.01-3.0 V	57.3 %	692 mA h g^{-1}	797 mA h g^{-1} after 150 cycles at 0.89 A g^{-1} (86.8%)
Ref.S15[15]	ZnO nanoparticles	plasma treatment	0.001-3.0 V	70.2 %	961 mA h g^{-1}	760 mA h g^{-1} after 100 cycles at 0.2 A g^{-1} (79.1%)
Ref.S16[16]	Amorphous MnO_x/C	aerosol spray pyrolysis	0.01-3.0 V	60.0 %	650 mA h g^{-1}	601 mA h g^{-1} after 130 cycles at 0.2 A g^{-1} (92.5%)
Ref.S17[17]	MnO@ Carbon composites	annealing treatment	0.01-3.0 V	59.1 %	738 mA h g^{-1}	660 mA h g^{-1} after 1000 cycles at 0.5 A g^{-1} (89.4%)
Ref.S18[18]	MnO/N-C hybrid	thermal calcination	0.01-3.0 V	73.7 %	884 mA h g^{-1}	667 mA h g^{-1} after 500 cycles at 0.5 A g^{-1} (75.5%)
Ref.S19[19]	Carbon coated TiO_2@ Fe_2O_3	template-assisted hydrolysis	0.01-3.0 V	76.2 %	640 mA h g^{-1}	516 mA h g^{-1} after 200 cycles at 0.2 A g^{-1} (80.6%)
Ref.S20[20]	Fe_2O_3 nanofibers	thermal treatment	0.005-3.0 V	34.0 %	420 mA h g^{-1}	680 mA h g^{-1} after 50 cycles at 65 mA g^{-1} (61.8%)

References:

1. Y. J. Hong and Y. C. Kang, *Carbon*, 2015, **88**, 262-269.
2. B. Zhao, S.-Y. Huang, T. Wang, K. Zhang, M. M. F. Yuen, J.-B. Xu, X.-Z. Fu, R. Sun and C.-P. Wong, *J. Power Sources*, 2015, **298**, 83-91.
3. L. Mei, C. C. Li, B. H. Qu, M. Zhang, C. Xu, D. N. Lei, Y. J. Chen, Z. Xu, L. B. Chen, Q. H. Li and T. H. Wang, *Nanoscale*, 2012, **4**, 5731-5737.
4. X. Huang, J. Chen, H. Yu, R. Cai, S. Peng, Q. Yan and H. H. Hng, *J. Mater. Chem. A*, 2013, **1**, 6901-6907.
5. J. Guo, H. Zhu, Y. Sun, L. Tang and X. Zhang, *J. Mater. Chem. A*, 2016, **4**, 16101-16107.
6. J. Lin, Z. W. Peng, C. S. Xiang, G. D. Ruan, Z. Yan, D. Natelson and J. M. Tour, *ACS Nano*, 2013, **7**, 6001-6006.
7. X. Shi, S. Liu, B. Tang, X. Lin, A. Li, X. Chen, J. Zhou, Z. Ma and H. Song, *Chem. Eng. J.*, 2017, **330**, 453-461.
8. Z. Chen, M. Zhou, Y. Cao, X. Ai, H. Yang and J. Liu, *Adv. Energy Mater.*, 2012, **2**, 95-102.
9. A. Jahel, C. M. Ghimbeu, L. Monconduit and C. Vix-Guterl, *Adv. Energy Mater.*, 2014, **4**, 1400025.
10. X. Li, X. Meng, J. Liu, D. Geng, Y. Zhang, M. N. Banis, Y. Li, J. Yang, R. Li, X. Sun, M. Cai and M. W. Verbrugge, *Adv. Funct. Mater.*, 2012, **22**, 1647-1654.
11. C. Guan, X. Wang, Q. Zhang, Z. Fan, H. Zhang and H. J. Fan, *Nano Lett.*, 2014, **14**, 4852-4858.
12. L. P. Wang, Y. Leconte, Z. Feng, C. Wei, Y. Zhao, Q. Ma, W. Xu, S. Bourrioux, P. Azais, M. Srinivasan and Z. J. Xu, *Adv. Mater.*, 2017, **29**.
13. X. Zhou, L.-J. Wan and Y.-G. Guo, *Adv. Mater.*, 2013, **25**, 2152-2157.
14. G.-P. Kim, S. Park, I. Nam, J. Park and J. Yi, *J. Mater. Chem. A*, 2013, **1**, 3872.
15. Y. Zhang, Y. Lu, S. Feng, D. Liu, Z. Ma and S. Wang, *J. Mater. Chem. A*, 2017, **5**, 22512-22518.
16. J. Guo, Q. Liu, C. Wang and M. R. Zachariah, *Adv. Funct. Mater.*, 2012, **22**, 803-811.
17. X. Li, S. Xiong, J. Li, X. Liang, J. Wang, J. Bai and Y. Qian, *Chem. - Eur. J.*, 2013, **19**, 11310-11319.
18. W. Zhang, J. Sheng, J. Zhang, T. He, L. Hu, R. Wang, L. Mai and S. Mu, *J. Mater. Chem. A*, 2016, **4**, 16936-16945.
19. J. Luo, X. Xia, Y. Luo, C. Guan, J. Liu, X. Qi, C. F. Ng, T. Yu, H. Zhang and H. J. Fan, *Adv. Energy Mater.*, 2013, **3**, 737-743.
20. M. V. Reddy, T. Yu, C. H. Sow, Z. X. Shen, C. T. Lim, G. V. Subba Rao and B. V. R. Chowdari, *Adv. Funct. Mater.*, 2007, **17**, 2792-2799.